Proceedings of the 2007 IEEE Symposium on Artificial Life (CI-ALife 2007)

Understanding and Harnessing Self-Organization

Cristina Costa Santini, Andy Tyrrell
The Intelligent Systems Group, Department of Electronics
University of York, York YO10 5DD UK
Email: ccs500@york.ac.uk

***Abstract*— A nonlinear dynamical system that exhibits limit cycle behaviour is investigated through numerical simulations of cardiac cells. This system's self-organizing behaviour is characterized aiming at harnessing it in an artificial system. Results of circuit simulations for different configurations of an architecture based on simple electronic elements are shown, characterizing self-organization in an artificial electronic circuit.**

I. Introduction

Some systems exhibit properties like robustness and adaptivity due to their self-organizing behaviour. These are desired properties in artificial systems. This paper aims at understanding this behaviour and at investigating how it could be harnessed in an artificial electronic circuit.

Self-organization and synchronization are phenomena exhibited by dynamical nonlinear systems. In these systems, the overall behaviour cannot be understood, predicted or accounted for by the behaviour exhibited by the individual parts of the system. "Classical" examples of this non-compartimentalization can be found throughout a variety of diverse environments and disciplines, in animate and inanimate matter; from the group behaviour exhibited by ants that cannot be understood by studying each ant individually to the operation of a laser and the supercondutivity of Josephson junctions.

So how might we understand, interact with and harness these systems that cannot be understood by simply looking at the individual parts? Most nonlinear systems cannot be understood analytically. However, state space analysis can offer qualitative understanding about the behaviour and the interactions between the variables.

Nonlinear systems are described (mainly) by their system variables and control parameters [1]. The former are also called dynamic variables and they evolve, change over time; the latter are also called boundary conditions and they define how these systems variables will change over time. In this way, exactly the same system can exhibit completely different behaviour over time depending on the control parameters. For example, take a nonlinear system described by 2 competing variables. For one set of boundary conditions these 2 variables will come to a fixed, stable solution (e.g. V1=5 and V2=4). For another set of boundary conditions there is no stable solution and these 2 variables will oscillate forever, in what is called a limit cycle. An additional concept that has to be introduced when discussing nonlinear systems is the initial condition, i.e., the value of the system variables when t=0. Given the same set of boundary conditions, the final behaviour of the system can be different depending on these initial conditions.

We narrow our focus to understand systems that exhibit rhythmic properties or limit cycles, such as excitable media. These systems are as diverse as chemical reactions and hepatocytes and share some common characteristics, namely self-organization and robustness. This is due to the fact that in these systems the overall behaviour, i.e. their functionality is not a result of the function of single elements but a consequence of the interaction of these elements.

The heart for example also exhibits these properties. It is robust, considering the diversity of influences that act upon it [2] but also adaptable to changes in the person's psychological and emotional state, physical workload and chemical balance [3]. Cardiac muscle can be seen as an excitable media as the qualitative behaviour of cardiac cells can be modeled by the FitzHugh-Nagumo (FHN) model, which is a generic model for excitable media.

In the work presented we show numerical simulations of a 2D grid of elements that represent 2 types of cardiac cells: a clump of self-oscillatory elements representing the Sinoatrial node (SAN) cells on an otherwise non-oscillatory medium representing the Atrial Myocardial (AM) cells. We investigate this system by measuring the phase synchronization effect of neighbouring cells for different coupling strengths: from independent to totally coupled cells.

The properties exhibited by these natural systems and theoretically characterized here are desirable in artificial systems. In electronic systems for example, components can function differently after some time or fail. Generally speaking, current methods are based on traditional architectures and are not robust to these faults. Different approaches to confer robustness to artificial systems are being studied [4]. Robustness would be specially important to Molecular Electronics architectures, where defect densities for bottom-up assemblies may be as high as a few percent [5][6]. It is in this context that we then investigate how these rhythmic systems' common self-organizing behaviour could be harnessed in an artificial system. We show circuit simulations of a 2D grid of circuit elements connected through resistive couplings and characterize this system for different coupling strengths.

This paper is organized as follows: In the next section we present our method for measuring the phase synchronization effect of neighbouring elements. In Section III we present the results for the numerical simulations of the grid composed of cardiac cells. In Section IV we present circuit simulations

for two circuit configurations and finally in Section V we conclude the paper discussing the results presented, suggesting applications and future work.

II. Measuring Phase Locking on the grid

Here we present our method for measuring phase synchronization on the nonlinear dynamical systems we investigate. These systems are typically composed of several parts or elements. We want to characterize these systems' dynamical behaviour in different conditions. (It is important to mention that our aim is not to fully characterize them as it has already been achieved for diverse systems and conditions [7][8][9][10].) The phase of the elements is calculated as [10][11]

$$\phi_i(t) = 2\pi \frac{t - \tau_k}{\tau_{k+1} - \tau_k} + 2\pi k \quad (1)$$

where τ_k is the time of the k-th firing of the element. This firing is defined by a threshold crossing of $x_i(t)$ at a suitable value depending on the simulation.

We characterize the phase synchronization effect of neighbouring elements on the grid by the quantity

$$s_{i,j} = sin^2\left(\frac{\phi_{i,j} - \phi_{i,j+1}}{2}\right) + sin^2\left(\frac{\phi_{i,j} - \phi_{i+1,j}}{2}\right), \quad (2)$$

where *i* represents the line of the element and *j* represents the column of the element on the grid. In this way the phase synchronization is measured in relation to the neighbour on the right and to the neighbour below.

A spatiotemporal average of $s_{i,j}$, i.e.,

$$S = \lim T \to \infty \frac{1}{T} \int_0^T \left(\frac{1}{N} \sum_{i=1,j=1}^{N} s_{i,j}\right) dt, \quad (3)$$

gives a measure of the degree of phase synchronization in the coupled system. For completely unsynchronized motion S≈0.5, while for globally synchronized system S≈0.

III. Cardiac Cells Simulation using The BVP Model

We investigate nonlinear dynamical systems that exhibit limit cycle behaviour through numerical simulations of cardiac cells. Cardiac muscle can be seen as an excitable media as the qualitative behaviour of cardiac cells can be modeled by the FitzHugh-Nagumo model [12], which is a generic model for excitable media and can be applied to a variety of systems. FitzHugh called his simplified model the Bon Hoeffer-van der Pol model (BVP) and derived it as a simplification of the Hodgkin-Huxley [13] equations. The model is able to reproduce many qualitative characteristics of electrical impulses along nerve and cardiac fibers and is described by the following pair of differential equations:

$$\frac{dx}{dt} = c(x + y - \frac{x^3}{3} + z) \quad (4)$$

$$\frac{dy}{dt} = -\frac{1}{c}(x - a + by), \quad (5)$$

where a, b and c are constants satisfying the relations

$$1 - \frac{2b}{3} < a < 1, 0 < b < 1, b < c^2 \quad (6)$$

and z is stimulating current. The coordinate x shares the properties of both membrane potential and excitability, while y is responsible for accomodation and refractoriness.

We use this model to simulate the qualitative behaviour of two types of cardiac cells as illustrated in Fig. 1: the SAN (sinoatrial node) cells, which are autonomous oscillators and the AM (atrial myocardial) cells, which are excitatory. The phase plane for (4) and (5) is shown in Fig. 2.

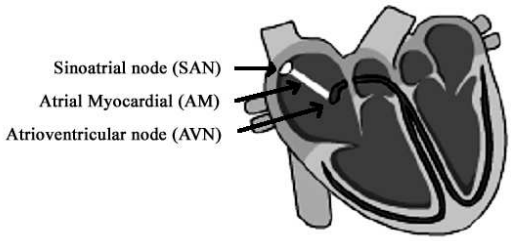

Fig. 1. Representation of the SAN cells that receive an stimulus from the autonomous nervous system, initiating an action potential that propagates through the AM to the AVN. The SAN cells are not identical, but nevertheless fire at the same frequency as they are phase locked.

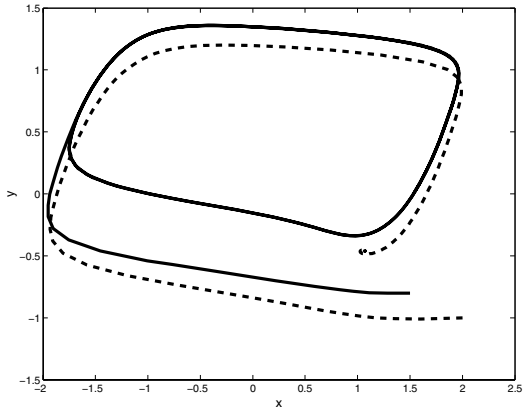

Fig. 2. BVP phase plane for a=0.7, b=0.8, c=3 in (4) and (5). In this simulation X represents the membrane potential and Y the recovery variable. The solid line corresponds to the oscillatory situation: a stable limit cycle for z=-0.4. The dashed line corresponds to an excitatory situation: the initial condition (x,y)=(2,-1) was taken to the fixed point for z=-0.2.

A. The Experimental Setup

We simulate a grid of 9x9 cardiac cells as depicted in Fig. 3. Each square shows the cells' membrane potential (x) as a function of time for independent, i.e. not coupled cells. The cells in the center represent the SAN cells. These are self-oscillatory and correspond to a limit cycle on the phase space as shown in Fig. 2. The other cells represent the AM cells. These are excitatory and therefore stable at their fixed point. Their phase space corresponds to the dashed line in Fig. 2.

Each cell corresponds to the pair of differential equations (4) and (5). When coupled, they are connected to their four nearest neighbours through diffusion of membrane potential (x) with zero flux boundary conditions at the edges. The equations for $cell_{i,j}$ where *i* is its line and *j* its column on the grid are

$$\frac{dx_{i,j}}{dt} = c(x_{i,j} + y_{i,j} - \frac{x_{i,j}^3}{3} + z) + \quad (7)$$
$$d(x_{i-1,j} + x_{i+1,j} + x_{i,j-1} + x_{i,j+1} - 4x_{i,j})$$
$$\frac{dy_{i,j}}{dt} = -\frac{1}{c}(x_{i,j} - a + by_{i,j}). \quad (8)$$

Following physiological description [14], the 13 SAN cells at the center of the grid are weakly coupled when compared to the 69 excitatory AM cells. If *dp* represents the diffusion coefficient between SAN cells and *d* represents the diffusion coefficient between AM cells, this means that *dp* is smaller *d*. (At the boundary between the two regions, i.e. between AM and SAN cells the coefficient is set to *d*.)

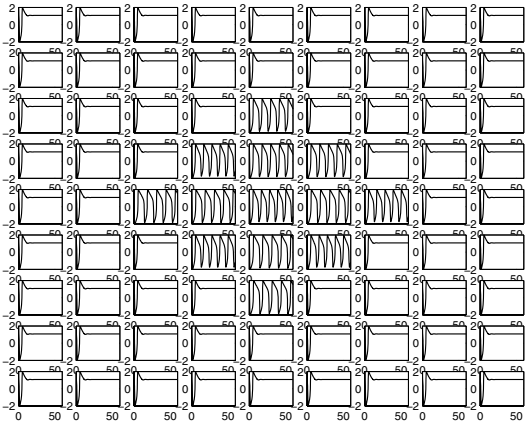

Fig. 3. Grid of 9x9 cardiac cells. Each square shows the cells' membrane potential (x) in time for independent cells. The cells in the center represent the SAN cells and are self-oscillatory whereas the other cells represent the AM cells and are excitatory.

It is important to point out that, as in the heart, these SAN cells are not identical. When independent, i.e. not coupled, they fire at different frequencies as illustrated in Fig. 4a. When coupled through diffusion (here *dp*=0.1 and *d*=0.3), the SAN cells are phase locked, as shown in Fig. 4b, and the AM cells propagate the stimulus, as shown in Fig. 4d.

B. Measuring Phase Locking and Synchronization

In order to characterize synchronization on an excitable system several parameters can be varied. Specifically in our example, where we model the behaviour of a clump of oscillatory cells in an otherwise non-oscillatory medium [14] aiming at investigating two types of cardiac cells, we could vary:

- the size of the oscillatory area (set to 13 SAN cells);
- the size of the non-oscillatory area (set to 69 AM cells);
- the excitability of these cells (e.g. z=-0.4 for the SAN cells and z=-0.2 for the AM cells).

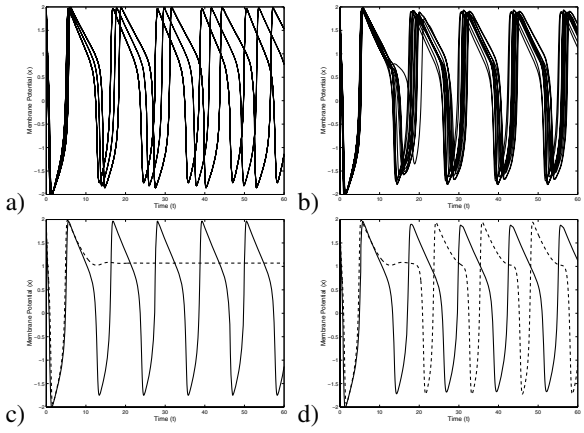

Fig. 4. Membrane potential (x) of the a) 13 independent SAN self-oscillatory cells firing at different frequencies; b) SAN cells coupled with *dp*=0.1 and phase locked c) AM cell (dashed line) on its fixed point for the uncoupled grid and d) AM cell conducting the stimulus when the cells are coupled (*dp*=0.1 and *d*=0.3).

However, here we fix these parameters as we are interested in determining the effect of the coupling strength, i.e. the effect of the level of interaction among the cells, on the synchronization of the grid. We measure the phase synchronization effect of neighbouring cells (*S* in (3)) for different coupling strengths (*dp* and *d* in (7)).

The graphs in Fig. 5 show these results. In Fig. 5a the diffusion between the SAN cells is constant (*dp*=1). We measure *S* for different diffusion coefficients between the AM cells ($0<d<1$). The dashed line shows the phase synchronization effect of neighbouring cells between all the cells on the grid whereas the solid line show this measure only between the SAN cells.

One can see that when the coupling is too weak ($d<0.2$) the stimulus does not propagate. Therefore, even though there is synchronization between the SAN cells (solid line $S< 0.05$), there is no synchronization on the grid (dashed line $S> 0.4$). On the other hand, when the coupling is too strong, ($d>0.5$), the stimulus is "washed away" and synchronization is lost on the grid as well as between the SAN cells.

There is then a well defined region of coupling strength where the synchronization on this excitable system is maintained, i.e. for $0.2<d<0.5$, $0.06>S>0.2$.

In Fig. 5b the diffusion between the AM cells is now constant (*d*=0.3) and we measure the phase synchronization for different diffusion values between the SAN cells ($0<dp<1$). One can see that there is a critical point, a critical value of coupling strength (*dp*=0.1) below which the oscillation on the SAN cells is not synchronized and therefore the propagation of the stimulus is not synchronized either.

These results characterize a self-organizing behaviour, as according to Sole [2], the characteristics signatures of SO would include:

- the creation of spatiotemporal structures in an initially homogeneous medium;

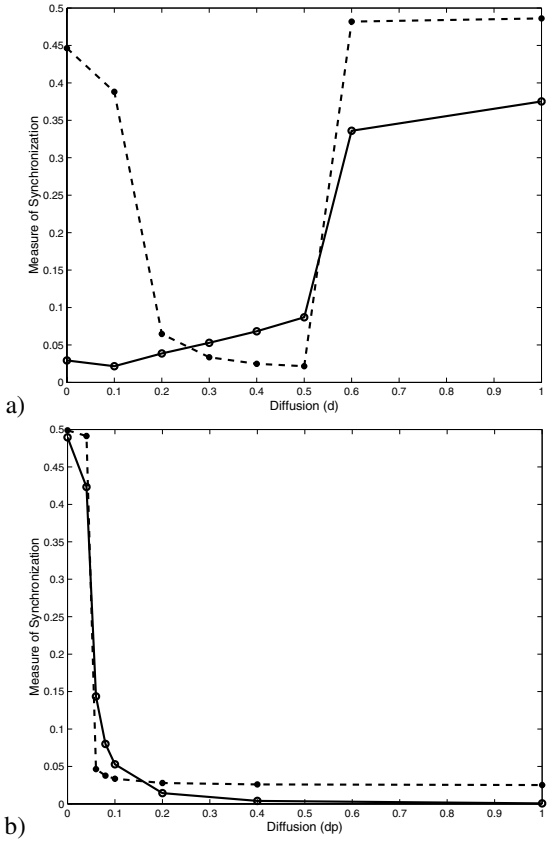

Fig. 5. Measure of the synchronization effect of neighbouring elements S for different coupling strengths when a) the diffusion between the SAN cells dp=0.1 and b) the diffusion between the AM cells d=0.3. The solid line shows S measured between the SAN cells and the dashed line shows S measured between all the cells on the grid.

- the possible existence of several stable states (multistability) and
- the existance of bifurcations when some parameters are varied: the behaviour of a self-organized system changes dramatically at bifurcations.

In this context, the specific details of single individuals will be rather irrelevant.

This self-organizing behaviour confers robustness and adaptativity to the heart. It is due to the interaction between the cells that some cardiac arrhythmias, for example, cause little disruption to the ability of the cardiac muscle to pump blood.

Could this self-organizing behaviour be harnessed on artificial systems, as we would like them to exhibit robustness and adaptivity?

As we did here for the numerical simulations of cardiac cells, we want to characterize self-organization on an artificial system. Therefore, in the next section, we present the results for the simulations of an electronic circuit.

IV. The Equivalent Circuit

Aiming at harnessing self-organization and the consequent properties of robustness and adaptativity in an artificial system, in this section we show the results for circuit simulations of an architecture based on simple electronic elements for different configurations.

An electronic simulator of the BVP model was first suggested by Nagumo [15]. We simulate a grid composed of 81 of these circuit elements as shown in Fig. 6. Results for two circuit configurations are presented: i) an oscillatory/excitatory grid, with monostable elements [15] and ii) an oscillatory grid with bistable elements [16]. We used LTSpice/SwithcerCADIII [17] in these circuit simulations.

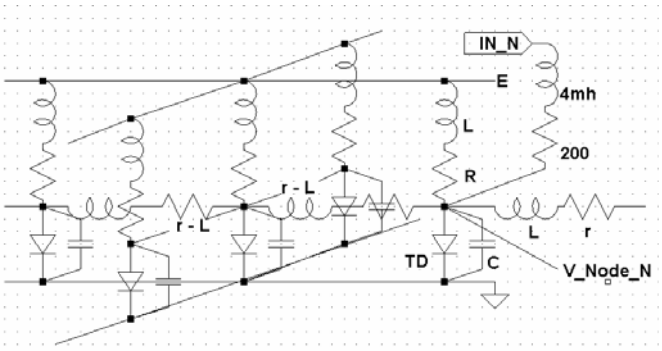

Fig. 6. Circuit Architecture. Each element or 'circuit node' comprises of a tunnel diode (TD), a capacitor (C), an inductor (L) and a resistor (R). These nodes are connected through a resistor (r) and an inductor (L) with zero flux boundary conditions at the edges.

A. The Oscillatory/Excitable Grid

As in the previous numerical simulation, here the circuit has been configured so that the 13 elements in the center of the grid are self-oscillatory and all other elements are excitatory (as depicted on the grid in Fig. 3). The parameters of the circuit elements in Fig. 6 for this configuration are: C=0.05μf, L=4mh, R=115Ω and E=150mV. The characteristic curve of the tunnel diode (TD) for these parameters is shown in Fig. 7.

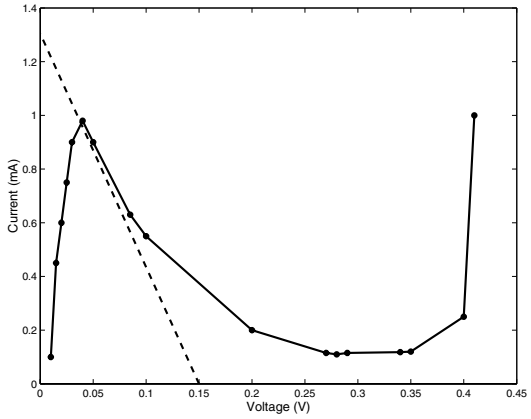

Fig. 7. Characteristic Curve of the tunnel diode (TD) with R=115Ω and E=150mV.

We investigate this circuit when its elements are connected in four different coupling situations as presented in Table I,

TABLE I
MEASURE OF PHASE SYNCHRONIZATION (*S*) ON THE OSCILLATORY/EXCITABLE GRID

	Measure of phase synchronization	
	on the whole grid	between oscillatory elements
a) disconnected r=50000 rp=50000	-	0.516
b) only oscillatory elements connected r=50000 rp=500	-	0.082
c) all the elements connected r=2500 rp=500	0.077	0.057
d) only oscillatory disconnected r=2500 rp=50000	0.217	0.419

measuring the phase synchronization effect of neighbouring elements *S* of the whole grid, i.e. between the 81 circuit elements, as well as only between the 13 oscillatory elements.

As in the previous experiment with the cardiac cells where *d* denoted the diffusion between two AM cells, here *r* denotes the value of the resistor on the connection between two excitatory circuit elements whereas *rp* denotes the value of the resistor on the connection between two oscillatory elements.

Fig. 8 shows the potential (V) measured on the 81 nodes for the four coupling situations presented in Table I.

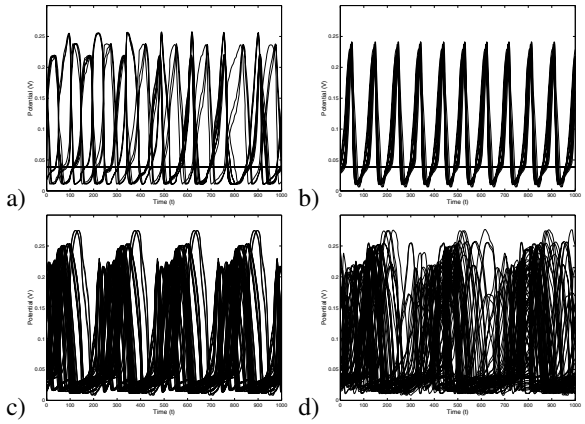

Fig. 8. Potential (V) measured on the 81 circuit elements' nodes for the 4 situations presented in Table I.

From these results, we observe that this grid's configuration would cause the excitatory elements to propagate the stimulus once for every two oscillations, showing a n:m entrainment [11]. Therefore, in order to measure the phase synchronization effect between neighbouring elements (2) becomes

$$s_{i,j} = sin^2(\frac{\phi_{i,j} - \frac{\phi_{i,j+1}}{2}}{2}) + sin^2(\frac{\phi_{i,j} - \frac{\phi_{i+1,j}}{2}}{2}), \quad (9)$$

when, for example, $cell_{i,j}$ is excitable whereas $cell_{i,j+1}$ and $cell_{i+1,j}$ are oscillatory.

When the grid is disconnected (Table I.a), the cells in the center fire with different frequencies (as they receive different initial inputs: 100, 120 or 140mV) whereas the other cells are stable at 40mV (they don't receive any input). This situation is presented in Fig. 8a. Then, by connecting only the 13 oscillatory elements we can observe that they synchronize (*S*=0.082), firing at the same frequency, as shown in Fig. 8b. Following this situation, we then connect all the elements on the grid. The oscillatory elements maintain the synchronization (*S*=0.057) and the other elements propagate the stimulus in an entrainment of 1:2 (*S*=0.077). If then the self-oscillatory elements are disconnected, they lose their synchronization (*S*=0.419) and consequently the entrainment on the grid is lost.

As we concluded for the numerical simulations of cardiac cells shown in Section III, these results also show that the oscillatory cells have to be synchronized for the propagation of the stimulus to be synchronized. In terms of robustness, we pointed out that in the heart, it is due to self-organization and the interaction between the cells that some cardiac arrythmias cause little disruption to the function of the heart. For the electronic circuit simulated here, in a situation like this where the grid shows entrainment and the stimulus is transmitted along the circuit nodes (Fig. 8c), it is straightforward to see that this transmission and consequently the overall function will not be affected if some elements are disconnected or faulty (open circuit), as the transmission will proceed through the neighbouring elements. However, the characterization of the robustness of this circuit, i.e. the number of elements that can be faulty without affecting its function, is subject other parameters such as the grid size and the circuit elements' characteristics.

B. The Oscillatory Grid

Inspired by the SAN cells that are autonomous oscillators, and by the fact that they are phase locked even though they are not identical, here we investigate the conditions for synchronization when this circuit is configured to have all its 81 elements self-oscillatory.

The parameters of the circuit elements in Fig. 6 are now C=0.05μf, L=4mh, R=500Ω and E=400mV. Consider the ideal situation when the homogeneous grid has R=500Ω and an input of 100mV on all its elements. The potential measured on all its 81 nodes for this situation is shown in Fig. 9. As all the elements are identical they fire together even being independent.

However, just as in the SAN case, where the cells are not identical, we want to investigate this grid with randomly varying circuit elements. Therefore the elements can have the resistance value R=480, 500 or 520Ω. The characteristic curve for these elements is shown in Fig. 10 with the three different load lines.

We simulate this nonhomogeneous grid of independent elements with R=480, 500 or 520Ω receiving 10 different randomly applied inputs varying from 96 to 114mV. Fig. 11

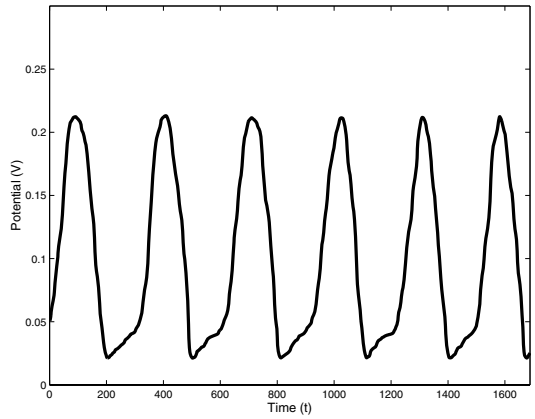

Fig. 9. Potential (V) measured on the 81 independent nodes for the perfect homogeneous grid.

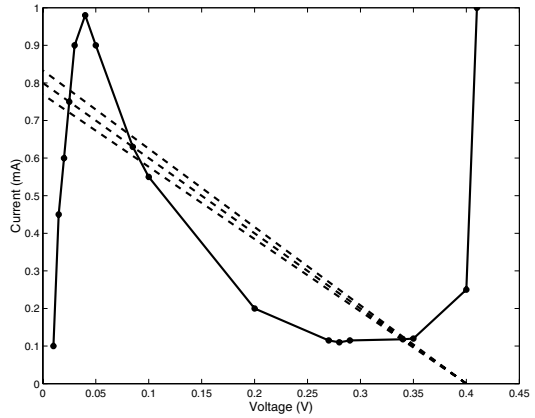

Fig. 10. Characteristic Curve of the tunnel diode with R=480Ω (dashed line on the top), R=500Ω and R=520Ω (bottom) and E=400mV.

shows the voltages measured on the 81 circuit elements' nodes in this situation.

We then investigate the synchronization on this grid for different resistive couplings (r in Fig. 6) measuring the phase synchronization effect of neighbouring elements *S* in (3) as well as the random global synchronization *Sg*, that we determine by

$$s_{h,j} = sin^2\left(\frac{\phi_{h,j} - \phi_{l,j}}{2}\right), \qquad (10)$$

where *h* for the 9x9 grid varies from 1 to 5, *l* from 6 to 9 and *j* from 1 to 9.

The spatiotemporal average of $s_{h,j}$

$$Sg = \lim T \rightarrow \infty \frac{1}{T}\int_0^T \left(\frac{1}{N}\sum_{i=1}^{N} s_i\right) dt, \qquad (11)$$

gives a measure of the degree of the random global phase synchronization in the coupled system, where N is the number of random elements *h,j*. The results shown here is for N=80.

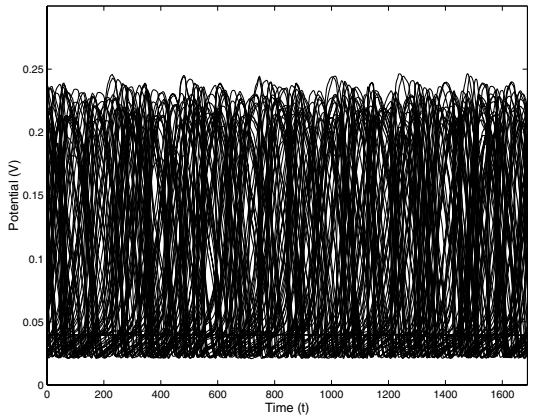

Fig. 11. Potential (V) measured on the 81 independent nodes on the grid with non-identical elements and noisy inputs.

The unsynchronized situation (r=50KΩ) shown in Fig. 11 can be compared to the synchronized situation shown in Fig. 12, when the elements are coupled through a resistor value r=200Ω. The measure of synchronization *S* and *Sg* for different resistive couplings is shown in Fig. 13. The results show that when r=50KΩ the coupling is too weak and the elements are independent, showing no synchronized behaviour. With a stronger coupling, (r≈10KΩ) there is no global synchronization (*Sg*≈0.45). However the nearest neighbour measure indicates that some clusters are synchronized (*S*=0.28). The critical value then for this specific circuit configuration is r=200Ω, below which there is no synchronization.

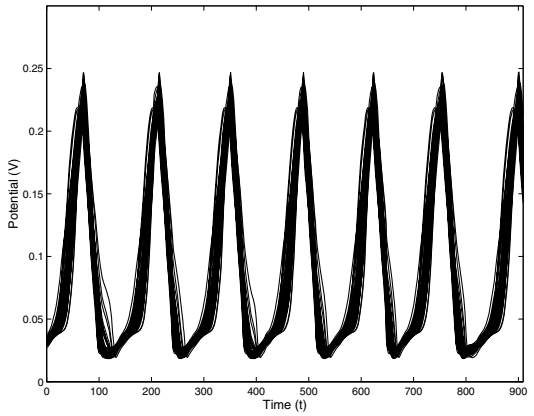

Fig. 12. Elements connected with r=200Ω. According to our method, the grid is completely synchronized, having the phase synchronization measure of neighbouring elements *S*=0.001884 and the global phase synchronization *Sg*≈0.012.

This result shows that synchronization could be maintained on a random grid with noisy inputs if the elements where set to interact within a specific range of coupling strength. As we mentioned for the numerical simulations of cardiac cells, these results for the circuit simulations presented here also characterize a self-organizing behaviour.

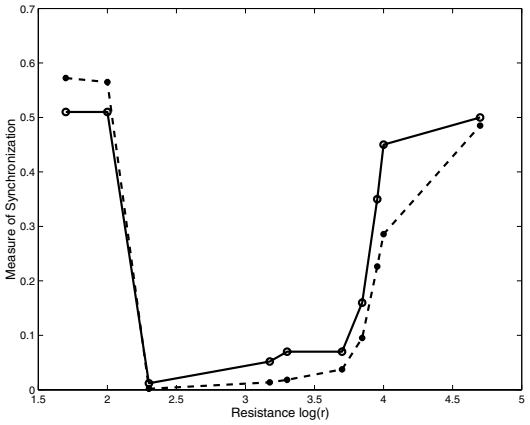

Fig. 13. The solid line shows the random global synchronization (*Sg*) and the dashed line shows the phase synchronization of neighbouring elements, (*S*) measured on the grid of 81 bistable oscillatory circuit elements.

V. Conclusion

This paper aims at understanding the self-organizing behaviour exhibited by a natural system and at investigating how it could be harnessed in an artificial one. The results presented show how the functioning of two types of cardiac cells can be qualitatively understood and measured in terms of self-organization. From this understanding we then investigate how self-organizing principles could be applied to engineering, on an oscillatory/excitatory grid as well as on a grid of bistable self-oscillatory circuit elements. Synchronization was demonstrated on the numerical simulation of cardiac cells and simularly obtained for the electronic circuit simulation for a certain range of resistive coupling between the circuit elements.

These results suggest self-organizing principles would be well applied on the design of architectures based on Molecular Electronic components. A major challenge to the implementation of these architectures is the fact that the specific performance of these elements can't be guaranteed, what makes current design approaches unsuitable for this substrate. An architecture that is intrisically robust to unreliable components would be desired [5]. Besides the fact that dynamical behaviour can then be exhibited by systems composed of unreliable components, according to the Complexity Engineering approach [18], this dynamical behaviour can be controlled and applied to problems where current design approaches don't present the optimal solution. These are typically systems that have to be adaptable (to an internal as well as an external changing environment), robust to hard and soft failures and flexible [19].

This dynamical nonlinear behaviour could also be applied to new computational paradigms. Take for example a computer chip, in which the electrical components are synchronized with a master clock. This centralized design has some disadvantages. 15 percent of the circuitry is wasted on distributing the clock signal and the clock itself consumes 20 percent of the power. But yet this centralized design is favored because of its simplicity, because traditionaly we know how to deal with centralized systems, whereas the alternative, many local clocks interacting with each other, would require a different perspective, a different approach, as well as more understanding about what is happening for example with cardiac pacemaker cells [20]. Self-organization offers new opportunities, by showing phenomena that are not a result of the function of the single elements but a consequence of the *interaction* of these elements.

Acknowledgment

The authors thank Jonas Buchli and Marcus Richards for discussions and review. C.C.S. is supported by the Programme Alban, the European Union Programme of High Level Scholarships for Latin America, scholarship no. E04D028324BR.

References

[1] S. Strogatz, *Nonlinear Dynamics and Chaos*. Addison Wesley Publishing Company, 1994.

[2] R. Sole and B. Goodwin, *Signs of Life: How Complexity Pervades Biology*. Basic Books, 2002.

[3] A. T. Winfree, *When Time Breaks Down: Three-Dimensional Dynamics of Electrochemical Waves and Cardiac Arrhythmias*. Princeton University Press, 1987.

[4] A. Tyrrell and H. Sun, "A honeycomb development architecture for robust fault-tolerant design," *First NASA/ESA Conference on Adaptive Hardware and Systems*, pp. 281– 287, 2006.

[5] M. R. Stan, P. D. Franzon, S. C. Goldstein, J. C. Lach, and M. M. Ziegler, "Molecular electronics: From devices and interconnect to circuits and architecture," *PROCEEDINGS OF THE IEEE3*, vol. 91, no. 11, pp. 1940–1957, 2003.

[6] C. M. Jeffery and R. J. O. Figueiredo, "Hierarchical fault tolerance for nanoscale memories," *IEEE Transactions on Nanotechnology*, vol. 5, no. 4, pp. 407–414, 2006.

[7] A. T.Winfree, "On emerging coherence," *Science*, vol. 298, pp. 2336–2337, 2002.

[8] I. Z. Kiss, Y. M. Zhai, and J. L. Hudson, "Emerging coherence in a population of chemical oscillators," *SCIENCE*, vol. 296, pp. 1676–1678, 31 May 2002.

[9] I. Z. Kiss and J. L. Hudson, "Phase synchronization of nonidentical chaotic electrochemical oscillators," *Phys. Chem. Chem. Phys.*, vol. 4, p. 26382647, 2002.

[10] B. Hu and C. Zhou, "Phase synchronization in coupled nonidentical excitable systems and array-enhanced coherence resonance," *PHYSICAL REVIEW E*, vol. 61, no. 2, pp. 1001–1004, 2000.

[11] A. Pikovsky, M. Rosenblum, J. Kurths, and B. Chirikov, *Synchronization: A Universal Concept in Nonlinear Sciences*, ser. Cambridge Nonlinear Science. Cambridge University Press, 2003.

[12] R. Fitzhugh, "Impulses and physiological states in theoretical models of nerve membrane," *Biophysical Journal*, vol. 1, pp. 445–466, 1961.

[13] A. L. Hodgkin and A. F. Huxley, "A quantitative description of membrane current and its application to conduction and excitation in nerve," *Journal of Physiology*, vol. 117, pp. 500–544, 1952.

[14] J. Keener and J. Sneyd, *A Mathematical Physiology (Interdisciplinary Applied Mathematics S.)*. Springer-Verlag New York Inc., 2001.

[15] N. J., A. S., and Y. S., "An active pulse transmission line simulating nerve axon," *Proc. IRE*, vol. 50, pp. 2061–2070, 1962.

[16] ——, "Bistable transmission lines," *Circuits and Systems, IEEE Transactions on*, vol. 12, pp. 400– 412, 1965.

[17] "Ltspice/switchercadiii v2.18," http://www.linear.com/.

[18] J. Buchli and C. C. Santini, "Complexity engineering - harnessing emergent phenomena as opportunities for engineering," *Project Report of the Santa Fe Institute's Complex Systems Summer School 2005*, 2005.

[19] J. Buchli, L. Righetti, and A. Ijspeert, "Engineering entrainment and adaptation in limit cycle systems," *Biological Cybernetics*, 2006, in press.

[20] S. Strogatz, *Sync: The Emerging Science of Spontaneous Order*. Penguin Books Ltd, 2004.